END

DATE
FILMED
3 - 77

MICROCOPY RESOLUTION TEST CHART

NATIONAL BUREAU OF STANDARDS-1963-A

AD

THE EFFECT OF THE K_α DOUBLET DIFFRACTED PEAK POSITION ON THE PRECISION OF THE LATTICE CONSTANT

CHARLES P. GAZZARA
METALS RESEARCH DIVISION

November 1976

ARMY MATERIALS AND MECHANICS RESEARCH CENTER
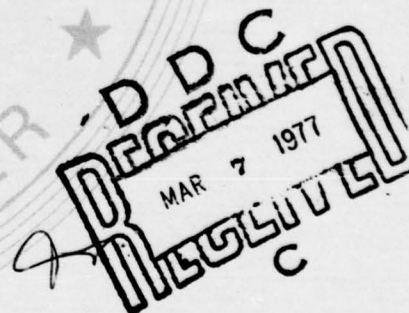Watertown, Massachusetts 02172

The findings in this report are not to be construed as an official Department of the Army position, unless so designated by other authorized documents.

Mention of any trade names or manufacturers in this report shall not be construed as advertising nor as an official indorsement or approval of such products or companies by the United States Government.

REPORT DOCUMENTATION PAGE		READ INSTRUCTIONS BEFORE COMPLETING FORM
1. REPORT NUMBER AMMRC-TR-76-37	2. GOVT ACCESSION NO.	3. RECIPIENT'S CATALOG NUMBER
4. TITLE (and Subtitle) THE EFFECT OF THE Kα DOUBLET DIFFRACTED PEAK POSITION ON THE PRECISION OF THE LATTICE CONSTANT.		5. TYPE OF REPORT & PERIOD COVERED Final Report
		6. PERFORMING ORG. REPORT NUMBER
7. AUTHOR(s) Charles P. Gazzara		8. CONTRACT OR GRANT NUMBER(s)
9. PERFORMING ORGANIZATION NAME AND ADDRESS Army Materials and Mechanics Research Center Watertown, Massachusetts 02172 DRXMR-EM		10. PROGRAM ELEMENT, PROJECT, TASK AREA & WORK UNIT NUMBERS D/A Project: 1T161102AH42 AMCMS Code: 611102.11.H4200
11. CONTROLLING OFFICE NAME AND ADDRESS U. S. Army Materiel Development and Readiness Command, Alexandria, Virginia 22333		12. REPORT DATE November 1976
		13. NUMBER OF PAGES 11
14. MONITORING AGENCY NAME & ADDRESS(if different from Controlling Office)		15. SECURITY CLASS. (of this report) Unclassified
		15a. DECLASSIFICATION/DOWNGRADING SCHEDULE

16. DISTRIBUTION STATEMENT (of this Report)

Approved for public release; distribution unlimited.

17. DISTRIBUTION STATEMENT (of the abstract entered in Block 20, if different from Report)

18. SUPPLEMENTARY NOTES

Presented at the 25th Annual Denver X-Ray Conference, Denver, Colorado, 5 August 1976.

19. KEY WORDS (Continue on reverse side if necessary and identify by block number)

X-ray diffraction	Yttrium aluminum garnet (YAG)
Lattice parameters	Precision
Silicon powder	

20. ABSTRACT (Continue on reverse side if necessary and identify by block number)

(SEE REVERSE SIDE)

Block No. 20

K sub alpha 1 - K sub alpha 2

ABSTRACT

The effect of the position of the X-ray unresolved K_{α_1} - K_{α_2} line doublets, diffracted from powder specimens, on the precision of the calculated lattice constant has been determined using a least-squares analysis. An analytical procedure to synthesize CuK_α doublet X-ray diffraction peaks with X-ray characteristic lines (half widths ranging from 0.1° to 0.4° 2θ) has been applied in correcting the weighted wavelength of the doublet peak position. A series of correction curves was established from which the true 2θ peak position of the weighted K_α wavelength could be determined from the measured 2θ peak position.

Data taken from silicon powder and an yttrium aluminum garnet (YAG) powder standard to calculate the lattice constants indicate:

a. A loss in precision of approximately one part in 25,000 in determining the lattice constant is obtained when calculated using doublet 2θ peak positions applied in the conventional manner (λ weighted = 1.54178 Å, at peak, for copper).

b. An increase in precision is obtained by using low as well as high 2θ angle diffraction peaks for calculating the lattice constant.

The effect of the measured characteristic line width, simulated by modifying the slit system, on the calculated lattice constant was determined in the case of the YAG powder specimen.

Suggestions to increase the precision of the lattice constants determined from X-ray diffraction powder samples are presented.

INTRODUCTION

The determination of the lattice constant a_0 of a unit cell, using the positions of characteristic X-ray lines diffracted from a powder sample, has been treated by many investigators. Calculations of the lattice constant made by extrapolating d values against various functions of the Bragg angle θ have been made using a least-squares analysis. A summary of the systematic error functions associated with an X-ray diffractometer has been presented by Vassamillet and King (1), who found that the best precision to be expected using a commercial diffractometer is approximately 1:20,000.

A comprehensive procedure that has been developed by Mueller, Heaton and Miller (2) (MHM method) involves varying the systematic error functions and computing the change in d for each systematic error function, or combination of functions, until the error in the computed lattice constant has been reduced to an acceptable level.

In a study (3) of the systematic errors involved in the computation of a_0 for yttrium aluminum garnet powder $Y_3Al_5O_{12}$ (YAG), it was found that the precision of the computed lattice constant was a function of the following.

(1) The slope of the least-squares straight line of the a_i values, where a_i is the lattice constant computed for each diffraction line, versus $\cot\theta_i$. A slope value of 0 indicated that the systematic errors had been adequately corrected for and yielded the most precise a_0 values.

(2) A statistical error term, i.e., standard error, absolute average deviation, rms deviation of functions of a_i and $\sin\theta_i$ from their computed functions or other error terms. A comparison of these error functions ultimately yield the same lattice constant. Whereas a difference was seen between error functions, their relative values were useful in establishing the same most precise a_0 values.

(3) The number and selection of the diffraction peaks. Using all 35 diffraction peaks (unresolved K_{α_1} - K_{α_2} doublets and high-angle resolved peaks) yielded the highest error. Restricting the analysis to the 12 highest 2θ angle peaks resulted in a reduction of 8% in error. Taking the 20 highest 2θ angle peaks increased the precision, reducing the error 28%. The fourth case gave the highest precision (42% reduction in error term), and occurred when 23 high- and low-2θ angle peaks were chosen, eliminating those doublet peaks in mid-2θ range, along with the diffracted peaks of low intensity.

1. VASSAMILLET, L. F. and KING, H. W. *Precision X-Ray Diffractometry Using Powder Specimens* in Advances in X-Ray Analysis, W. M. Mueller et al., ed., v. 6, Plenum Press, New York, 1963, p. 142-157.
2. MUELLER, M. H., HEATON, L., and MILLER, K. T. *Determination of Lattice Parameters with the Aid of a Computer.* Acta Cryst., v. 13, 1960, p. 828-829.
3. GAZZARA, C. P. *The Effect of Systematic Errors on the Measurement of Lattice Constants.* Army Materials and Mechanics Research Center, AMMRC TR 70-29, September 1970.

Recently, in an attempt to relate the peak height to the integrated intensity of X-ray diffracted K_α doublets by convoluting the characteristic peaks, it was found that the weighted K_α wavelength approximation was inaccurate except at very low Bragg angles (4). It therefore seemed appropriate to determine what the effect of this doublet peak position error would be in computing the lattice constant of a material whose lattice constant was known and to afford a means for correcting for the doublet position.

PROCEDURE

A doublet peak position correction curve could be generated for CuK_α radiation from the curve shown in Figure 1 (4), relating the value of the positional parameter X_1 of the analytical expressions describing the K_{α_1} and K_{α_2} lines to a, the function defined as the K_{α_1} - K_{α_2} peak separation in terms of the wavelength dispersion. Note that it is only in the linear portion of the curve, that the weighted K_α peak position approximation is valid (i.e., $X_1 = a/3$).
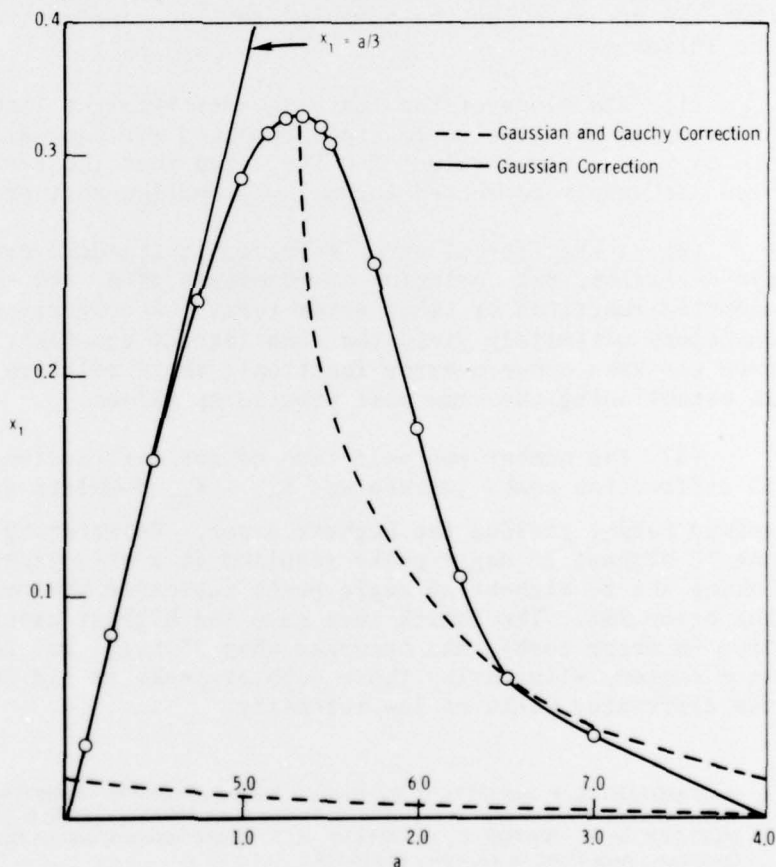

Figure 1. Plot of positional parameter X_1 versus CuK_{a_1} · CuK_{a_2} diffracted peak separation a, assuming Gaussian and Gaussian plus Cauchy distribution.

4. GAZZARA, C. P. *Peak Height Approximation for X-Ray Diffracted Integrated Intensity* in Advances in X-Ray Analysis, R. W. Gould, C. S. Barrett, J. B. Newkirk, and C. O. Ruud, ed., v. 19, Kendall Hunt, Iowa, 1976, p. 735-748.

The solid curve in Figure 1 was generated assuming a Gaussian distribution of the K_{α_1} and K_{α_2} diffraction peaks as a function of θ. The dashed curve was computed by fitting a computed characteristic K_{α_1} peak to an experimental CuK_{α_1} (531) Si diffraction peak, where the upper half was assumed to be Gaussian and the lower half to have a Cauchy distribution (Gaussian and Cauchy).

It can be shown that the equation relating the change in wavelength to a or X_1a is:

$$\Delta\lambda = \lambda a \omega_{h_{\frac{1}{2}}}/4.72 \tan\theta$$

where $\omega_{h_{\frac{1}{2}}}$ is the characteristic peak width at half peak height. Values of $\omega_{h_{\frac{1}{2}}}$ can be obtained from Figure 2 from the measured peak width at half height of the unresolved K_α peak doublet $\omega_{T_{\frac{1}{2}}}$. A series of curves was generated, see Figure 3, relating the 2θ doublet peak position to the t correction term whereby

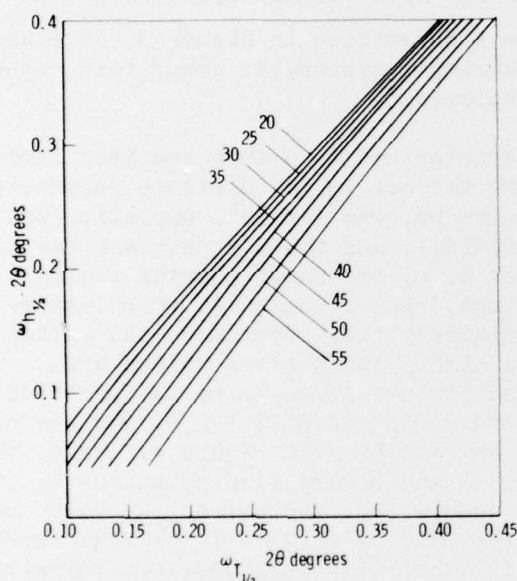$$2\theta_{corrected} = 2\theta_{measured} + t.$$

Figure 2. $\omega_{h_{1/2}}$ versus $\omega_{T_{1/2}}$ curves calculated for various levels of 2θ from 20° to 55° assuming Gaussian and Cauchy peak distributions.

Figure 3 is also made up of solid lines relating to Gaussian diffraction peaks while the dashed curves were calculated assuming a Gaussian and Cauchy characteristic diffraction line.

To determine the effect such a t correction would have on the lattice constant precision, CuK_α diffraction peak positions of silicon powder were measured. A CuK_α powder pattern of silicon powder with a particle size of less than 30 microns was taken with a 0.05° receiving
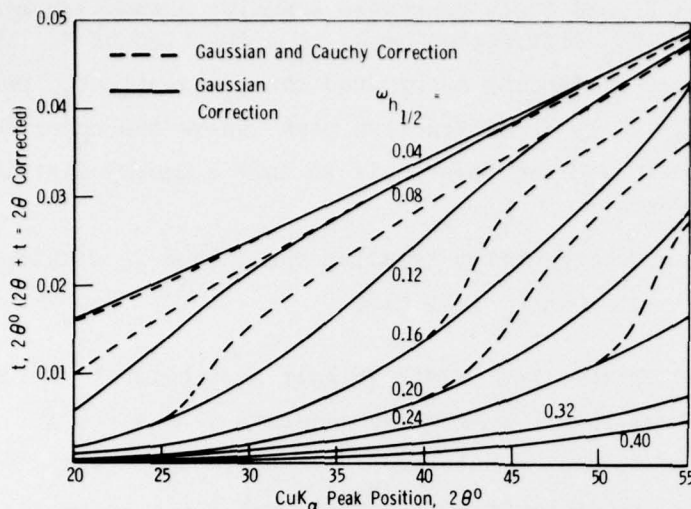
3

Figure 3. Plots of peak correction term t versus observed diffracted 2θ peak position of CuK_α doublets for constant values of $\omega_{h_{1/2}}$.

slit. A scanning speed of $0.10°$ (2θ)/min and a $1°$ (2θ) beam slit was used on a G.E. XRD-5 X-ray diffractometer. For the first three diffraction peaks an $\omega_{h_{1/2}}$ value of approximately $0.13°$ 2θ was determined from Figure 2 and applied in deriving the t correction in Figure 3. A least-squares extrapolation procedure utilizing a systematic error term, $\cot\theta$, and a weighting factor, $\tan\theta$, was employed.

The plane of the Si powder, characterized as a thin specimen (less than 0.002" thick), was adjusted with respect to the distance perpendicular to the plane of the specimen. The purpose for this operation was to minimize the slope (slope = $\Delta a_i / \Delta \cot \theta_i$), and thereby increase the precision of the a_0 measurement. Values of a_i are shown plotted versus θ in Figure 4 for three specimen settings. For position A, which represents the ideal alignment for an infinitely thick specimen, the extrapolated value of a_0 at $\theta = 90°$ is too high. The plotted values and computed curves applying the t correction are shown below the uncorrected curves. The specimen was moved inward 0.005" to position B, and the effects of the least-squares computation are shown in Figure 4. Next, the calculated slope values for positions A and B were plotted versus a_0 (see Figure 5) and, following a known procedure (3), the correct a_0 value was determined for slope = 0. Using this value of a_0, position C was found by varying the specimen position until the (111) CuK_α peak was maximized at the proper 2θ value for slope = 0. Plotting values of a_i for position C are shown in Figure 4 and the respective calculated values of a_0 are shown in Figure 5. The computed results of this procedure are summarized in Table 1.

Since a prior study of lattice constant measurements was performed with YAG powder, it was next deemed appropriate to ascertain the effects of the t correction on a YAG powder, where:

4

Table 1. SILICON LATTICE CONSTANT VALUES MEASURED FROM
THIN SPECIMEN AS A FUNCTION OF SPECIMEN DISPLACEMENT

(Powder Size Less Than 30 µM, 0.05° Receiving Slit,
1° Beam Slit, 0.10°/Min Scan Speed)

Specimen Position	Number of Diffracted Peaks	t Correction	a_0, Å	Slope	Weighted RMS Deviation
A (aligned for thick specimen)	12	None	5.4323	-0.0038	0.00130
	12	Gaussian	5.4325	-0.0044	.00120
	12	Gaussian & Cauchy	5.4325	-0.0045	.00124
	9 High Angle	-	5.4322	-0.0035	.00083
B (specimen displaced 0.005" inwards)	12		5.4310	0.0043	0.00083
	12		5.4312	.0036	.00070
	12		5.4312	.0036	.00073
	9 High Angle		5.4310	.0043	.00028
C (specimen in optimum alignment)	12		5.4315	0.0008	0.00072
	12		5.4317	.0002	.00049
	12		5.4317	.0002	.00051
	9 High Angle		5.4316	.0007	.00034

a. many more diffraction peaks are available (12 Si → 35 YAG);

b. an accurate value of the lattice constant was available for the YAG powder;

c. the effect of $\omega_{h_{1/2}}$ and the lattice constant could be found by varying the receiving slit width, from 0.05° 2θ to 0.10° 2θ to 0.20° 2θ;

d. the case of using only the high angle diffraction peaks could be examined; and

e. unresolved K_α doublets beyond the 2θ correction range could be eliminated (this case denoted as m). For a 0.05° receiving slit, peak $\Sigma h^2 = 52$ was eliminated; for a 0.10° slit, peaks $\Sigma h^2 = 52, 54, 56$ were removed; and for a 0.20° slit peaks $\Sigma h^2 = 52$ to 88 were taken out of the least-squares analysis. The results of the analysis of the thin YAG powder specimen are summarized in Table 2.

RESULTS

The effect of the error in assigning a CuK_α wavelength of 1.54178 Å to the unresolved characteristic line doublet peak position, on the calculated lattice constant of either silicon or YAG always lowers the true value of a_0 by approximately one part in 25,000 (see Figure 5). It can also be seen from Table 1 and Figure 4 that the t correction is practically the same whether the K_{α_1} and K_{α_2} lines are considered to be Gaussian or Gaussian and Cauchy. It is also evident that with a t correction, the error terms decrease and the slope decreases when the systematic error function is properly treated. Table 1 and Figure 5 show the effect on the analysis resulting from eliminating the first three CuK_α silicon powder diffraction peaks and using the remaining nine higher angle peaks.
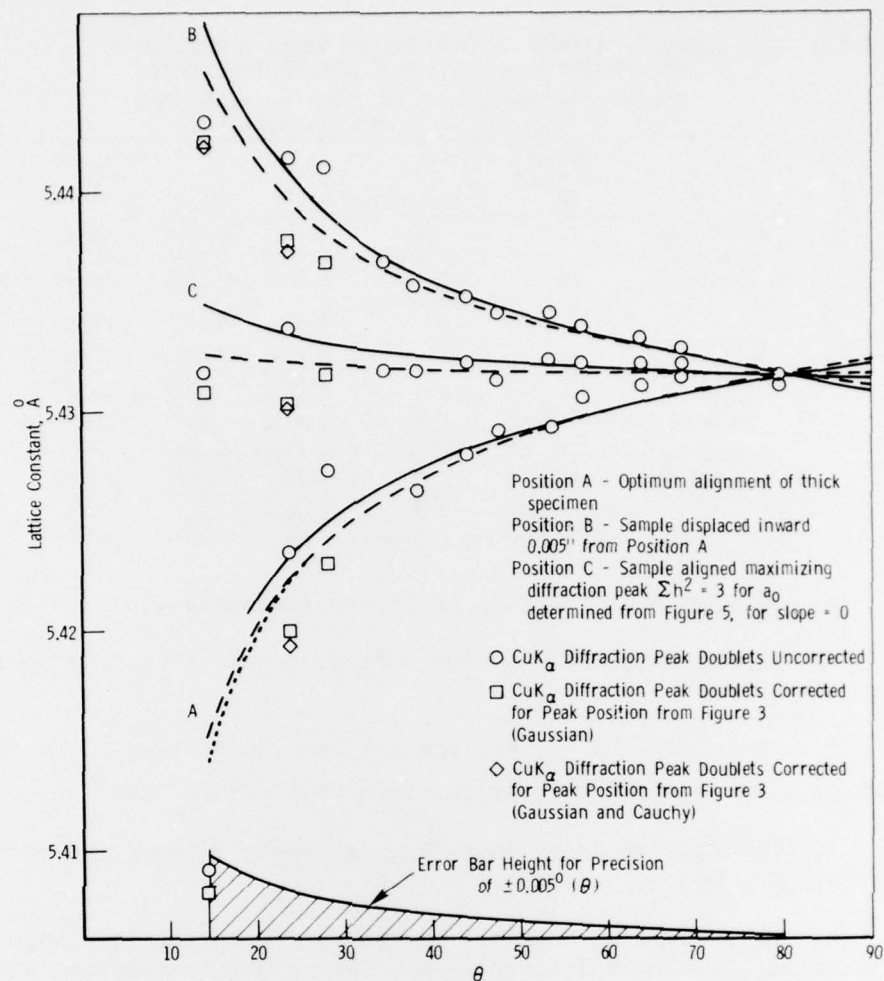
5

Figure 4. Values of lattice constant a_i calculated from diffracted peak position of family of planes $\{hkl\}_i$ versus Bragg angle θ for a thin silicon powder specimen.
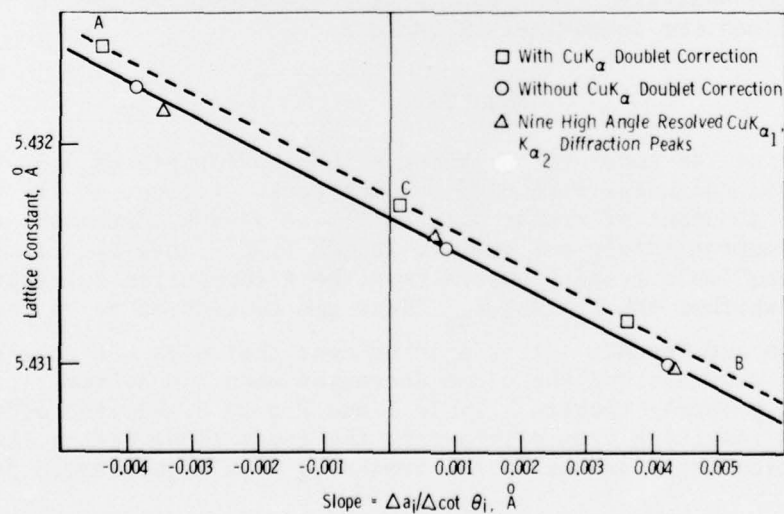
Position A - Optimum alignment of thick specimen

Position B - Sample displaced inward 0.005" from Position A

Position C - Sample aligned maximizing diffraction peak $\Sigma h^2 = 3$ for a_0 determined from Figure 5, for slope = 0

○ CuK_α Diffraction Peak Doublets Uncorrected

□ CuK_α Diffraction Peak Doublets Corrected for Peak Position from Figure 3 (Gaussian)

◇ CuK_α Diffraction Peak Doublets Corrected for Peak Position from Figure 3 (Gaussian and Cauchy)

Error Bar Height for Precision of $\pm 0.005^0$ (θ)

□ With CuK_α Doublet Correction

○ Without CuK_α Doublet Correction

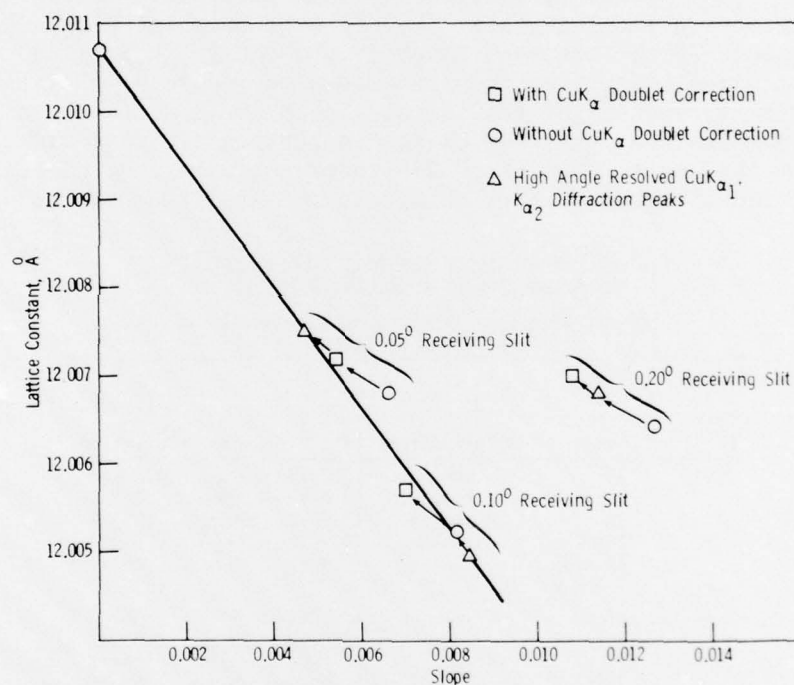△ Nine High Angle Resolved CuK_{α_1} K_{α_2} Diffraction Peaks

Figure 5. Lattice constant a_0 versus slope term for thin silicon powder specimen showing effect of t correction and the use of high angle diffraction peaks only.

6

The data points in Figure 5 are approximately the same as those obtained using all the diffraction peaks, without the t correction, in agreement with earlier work (3).

From Figure 4, notice the effect of improperly treating the systematic error in extrapolating to a_0. In this case an error of one part in 5000 in a_0 is possible, indicative of the importance of considering the slope term, unless a procedure such as the MHM method is employed.

The lattice constants computed from the experimental data obtained from the YAG powder may be seen in Table 2 and in the plot of Figure 6. The value of the lattice constant at slope = 0 was determined from an earlier MHM analysis to be 12.0107 Å (3).

In the case of YAG, it can be seen that the most precise values of a_0 are obtained with a $0.05°$ receiving slit, progressing from using the uncorrected K_α doublet peaks, to employing the t correction, to using the high angle peaks alone. These results represent the only conditions where the high angle data gave the best results, in conflict with earlier work (3). The lowest lattice constant values are obtained with the intermediate size receiving slit ($0.10°$) when only the high angle peaks are utilized. For both cases, however, the change in lattice constant with slope moves along the same line shown in Figure 6. For the $0.10°$ receiving slit, when eight additional mid-2θ angle diffraction peaks are removed from the analysis, the change in lattice constant with slope departs from the curve. For the $0.20°$ receiving slit, the slope values increase, indicating a further change in the magnitude of the systematic

Table 2. YAG LATTICE CONSTANT VALUES MEASURED
AS A FUNCTION OF RECEIVING SLIT SIZE

(Powder Size Less Than 30 μM, 1° Beam Slit,
0.10°/Min Scan Speed)

Receiving Slit ($2\theta°$)	Number of Diffracted Peaks	t Correction	a_0, Å	Slope	Weighted RMS Deviation
0.05	35	None	12.0068	0.0063	0.00347
	34(m)	None	12.0069	.0060	.00330
	35	Gaussian	12.0071	.0056	.00329
	34(m)	Gaussian	12.0072	.0053	.00305
	23 High Angle	-	12.0075	.0047	.00195
0.10	35		12.0052	0.0081	0.00380
	32(m)		12.0054	.0076	.00357
	35		12.0055	.0075	.00401
	32(m)		12.0057	.0070	.00371
	21 High Angle		12.0050	.0085	.00233
0.20	35		12.0064	0.0126	0.00417
	26(m)		12.0068	.0113	.00277
	35		12.0066	.0123	.00428
	26(m)		12.0070	.0108	.00280
	15 High Angle		12.0068	.0113	.00187

7

errors, with a displacement of the points from the curve. The error terms shown in Table 2 indicate no unusual behavior between cases except that in treating the 0.20° receiving slit case, the sensitivity of removing the mid-range diffraction peaks seems to be more severe. This is expected when one considers that the doublet correction t has not been taken into account, since these corrections occur beyond the angular range considered in Figure 3.

CONCLUSIONS

1. A correction for the 2θ X-ray diffracted peak position of CuK_α unresolved doublets results in an increase in lattice constants, calculated from a least-squares extrapolation procedure, of one part in 25,000 for silicon and YAG powder.

2. The same peak position of the unresolved K_α doublet results from assuming either a Gaussian or a Gaussian plus Cauchy distribution of the CuK_{α_1} and CuK_{α_2} X-ray diffraction lines.

Figure 6. Lattice constant a_0 versus slope term for thin YAG powder specimen showing the effect of t correction and the use of high angle diffraction peaks only.

3. In the absence of an extensive procedure such as that of MHM (2), an extrapolation procedure utilizing a plot of a_0 versus slope can be applied to minimize the effect of systematic errors and increase the precision in a_0.

8

4. The most precise values of a_0 are usually obtained when high- and low-2θ angle diffraction peaks are employed in a least-squares analysis. This is particularly true when few diffraction peaks are available, i.e., silicon powder with CuK_α. High precision can also be achieved when many diffraction peaks are available, i.e., YAG case, utilizing only the high 2θ angle diffraction peaks.

ACKNOWLEDGMENT

9

No. of Copies	To
2	Metals and Ceramics Information Center, Battelle Columbus Laboratories, 505 King Avenue, Columbus, Ohio 43201
12	Commander, Defense Documentation Center, Cameron Station, Building 5, 5010 Duke Street, Alexandria, Virginia 22314
	Office of Chief of Research and Development, Department of the Army, Washington, D. C. 20310
1	ATTN: CRDPES
1	Commander, Army Research Office, P. O. Box 12211, Research Triangle Park, North Carolina 27709
	Commander, U. S. Army Material Development and Readiness Command, 5001 Eisenhower Avenue, Alexandria, Virginia 22333
1	ATTN: DRCQA
2	DRCQA-E
2	DRCQA-P
1	DRCLDC, Mr. R. Zentner
1	DRCRL
1	DREDE-EA
1	DRCDE-E
1	DRCRP-OIP
	Commander, U. S. Army Electronics Command, Fort Monmouth, New Jersey 07703
2	ATTN: DRSEL-CB
1	DRSEL-PP-PO
1	DRSEL-WM
1	DRSEL-RD-GT
1	DRSEL-PA-C
	Commander, U. S. Army Missile Command, Redstone Arsenal, Alabama 35809
2	ATTN: DRSMI-RBLD, Redstone Scientific Information Center
1	DRSMI-RSM, Mr. E. J. Wheelahan
1	DRSMI-RTR, Mr. H. T. Lawson
2	DRSMI-Q
1	DRSMI-M
	Commander, U. S. Army Mobility Equipment Research and Development Command, 4300 Goodfellow Boulevard, St. Louis, Missouri 63120
1	ATTN: DRSME-Q
1	DRSME-QP
1	DRSME-QR
1	DRSME-QE
1	DRSME-M
1	DRSME-P
1	DRSME-R
	Commander, U. S. Army Armament Command, Rock Island, Illinois 61201
1	ATTN: DRSAR-SC, Dr. C. M. Hudson
1	DRSAR-PPW-PB, Mr. Francis X. Walter
2	Technical Library

No. of Copies	To

2 Commander, U. S. Army Natick Research and Development Command,
Kansas Street, Natick, Massachusetts 01760
1 ATTN: DRXNM-QE
1   DRXNM-GE

Commander, U. S. Army Tank-Automotive Research and Development Command,
28251 Van Dyke Avenue, Warren, Michigan 48090
1 ATTN: DRDTA-RXMT, Mr. J. Dudzinski
1   DRDTA-RXMT, Mr. F. Lemmer
1   DRDTA-RXMT, Mr. W. Wulf
1   DRDTA-RGD, Mr. O. Renius
2   DRDTA-QEE, Mr. P. Duika

Commander, U. S. Army Test and Evaluation Command, Aberdeen Proving Ground,
Maryland 21005
2 ATTN: DRSTE-TA-A

Commander, Aberdeen Proving Ground, Maryland 21005
1 ATTN: STEAP-MT, Mr. J. M. McKinley
1   STEAP-TL

Commander, Edgewood Arsenal, Edgewood, Maryland 21010
1 ATTN: SAREA-TSP
1   SAREA-QAE
1   SAREA-QAI
1   SAREA-QAP
1   SAREA-QAIP

Commander, U. S. Army Foreign Science and Technology Center,
220 7th Street, N. E., Charlottesville, Virginia 22901
1 ATTN: DRXST-SD2

Commander, Frankford Arsenal, Philadelphia, Pennsylvania 19137
1 ATTN: SARFA-P3300
1   SARFA-C2500
1   SARFA-Q1000
2   SARFA-Q2100
1   SARFA-N3100-202-1, Mr. E. Roffman
1   SARFA-Q6120-64-1, Mr. W. Shebest
1   SARFA-Q6130-64-1, Mr. G. Norwitz
1   SARFA-A2000
2   SARFA-F6000
1   SARFA-L300, Mr. J. Corrie

1 Commander, Harry Diamond Laboratories, 2800 Powder Mill Road,
Adelphi, Maryland 20783
2 ATTN: DRXDO-EDE

Commander, Picatinny Arsenal, Dover, New Jersey 07801
1 ATTN: SARPA-RT-S
1   SARPA-VA6, Mr. H. DeFazio
1   SARPA-VC2, Mr. T. M. Roach, Jr.
1   SARPA-VG, Mr. A. Clear
1   SARPA-ND 1, Mr. D. Stein
1   SARPA-FR-M-D, A. M. Anzalone, Bldg. 176

No. of Copies	To

Commander, Rock Island Arsenal, Rock Island, Illinois 61201
1 ATTN: SARRI-L, Dr. Royce Beckett
1   SARRI-LEQ
2   SARRI-LRM

Director, U. S. Army Production Equipment Agency, Rock Island Arsenal,
Rock Island, Illinois 61201
1 ATTN: DRXDE-MT

Commander, U. S. Army Aeronautical Depot Maintenance Center,
Corpus Christi, Texas 78419
1 ATTN: SSMAC-Q

Commander, U. S. Army Ammunition Procurement and Supply Agency,
Joliet, Illinois 60436
2 ATTN: SMUAT-E

2 Commander, U. S. Army Mobility Equipment Research and Development Command
   Fort Belvoir, Virginia 22060
1 ATTN: Technical Documents Center, Bldg. 315
1   DRXFB-P
1   DRXFB-M
1   DRXFB-X
1   DRXFB-A
1   DRXFB
1   DRXFB-B
1   DRXFB-H
1   DRXFB-J
1   DRXFB-F
1   DRXFB-MM
1   DRXFB-Q
1   DRXFB-QQ
1   DRXFB-QE, Mr. Jacob K. Mauzy
1   DRXFB-MW, Dr. J. W. Bond

2 Commander, Watervliet Arsenal, Watervliet, New York 12189
1 ATTN: SARWV-QA, Mr. J. Miller
1   SARWV-QA, Quality Assurance Office

Commander, Anniston Army Depot, Anniston, Alabama 36202
1 ATTN: AMXAN-QA

Commander, Atlanta Army Depot, Forest Park, Georgia 30050
1 ATTN: AMXAT-CSQ

Commander, Letterkenny Army Depot, Chambersburg, Pennsylvania 17201
1 ATTN: AMXLE-CQ
1   AMXLE-NSQ

Commander, Lexington-Bluegrass Army Depot, Lexington, Kentucky 40507
1 ATTN: AMXLX-QA

Commander, New Cumberland Army Depot, New Cumberland, Pennsylvania 17070
1 ATTN: AMXNC-256

Commander, Pueblo Army Depot, Pueblo, Colorado 81001
1 ATTN: AMXPU-BF

No. of Copies	To

Commander, Red River Army Depot, Texarkana, Texas   75502
1 ATTN: AMXRR-QAO

Commander, Sacramento Army Depot, Sacramento, California   95801
1 ATTN: AMXSA-QA

Commander, Savanna Army Depot, Savanna, Illinois   61074
1 ATTN: AMXSV-QAO

Commander, Seneca Army Depot, Romulus, New York 14541
1 ATTN: AMXSE-AXI

Commander, Sharpe Army Depot, Lathrop, California   95330
1 ATTN: AMXSH-CQ

Commander, Sierra Army Depot, Herlong, California   96113
1 ATTN: AMXSI-QA

Commander, Tobyhanna Army Depot, Tobyhanna, Pennsylvania   18466
1 ATTN: AMXTO-Q

Commander, Tooele Army Depot, Tooele, Utah   84074
1 ATTN: AMXTE-QAD

Commander, Umatilla Army Depot, Hermiston, Oregon   97838
1 ATTN: AMXUM-QA

1 Chief, Bureau of Naval Weapons, Department of the Navy,
Washington, D. C.   20390

1 Chief, Bureau of Ships, Department of the Navy, Washington, D. C.   20315

Naval Research Laboratory, Washington, D. C.   20390
1 ATTN: Dr. J. M. Krafft - Code 6305
2   Dr. G. R. Yoder - Code 6382

Commander, Wright Air Development Division, Wright-Patterson
Air Force Base, Ohio   45433
2 ATTN: ASRC
1   AFML/MBC/Mr. Stanley Schulman

Commander, U. S. Army Aviation Systems Command, St. Louis, Missouri   63166
1 ATTN: DRSAV-R-R
1   DRSAV-R-EGE
1   DRSAV-A-L
1   DRSAV-LE
1   DRSAV-A-LV
1   DRSAV-A-V

Director, Army Materials and Mechanics Research Center,
Watertown, Massachusetts   02172
2 ATTN: DRXMR-PL
1   DRXMR-AG
1   Author

Army Materials and Mechanics Research Center,
Watertown, Massachusetts 02172
THE EFFECT OF THE K_α DOUBLET DIFFRACTED
PEAK POSITION ON THE PRECISION OF THE
LATTICE CONSTANT - Charles P. Gazzara

Technical Report AMMRC TR 76-37, November 1976, 11 pp -
illus-tables, D/A Project 1T161102AH42,
AMCMS Code 611102.11.H4200

AD
UNCLASSIFIED
UNLIMITED DISTRIBUTION

Key Words

X-ray diffraction
Lattice parameters
Silicon powder

The effect of the position of the X-ray unresolved $K_{\alpha 1}$ - $K_{\alpha 2}$ line doublets, diffracted from powder specimens, on the precision of the calculated lattice constant has been determined using a least-squares analysis. An analytical procedure to synthesize CuK_α doublet X-ray diffraction peaks with X-ray characteristic lines (half widths ranging from 0.1° to 0.4° 2θ) has been applied in correcting the weighted wavelength of the doublet peak position. A series of correction curves was established from which the true 2θ peak position of the weighted K_α wavelength could be determined from the measured 2θ peak position. Data taken from silicon powder and an yttrium aluminum garnet (YAG) powder standard to calculate the lattice constants indicate: a) A loss in precision of approximately one part in 25,000 in determining the lattice constant is obtained when calculated using doublet 2θ peak positions applied in the conventional manner (λ weighted = 1.54178 Å, at peak, for copper). b) An increase in precision is obtained by using low as well as high 2θ angle diffraction peaks for calculating the lattice constant. The effect of the measured characteristic line width, simulated by modifying the slit system, on the calculated lattice constant was determined in the case of the YAG powder specimen. Suggestions to increase the precision of the lattice constants determined from X-ray diffraction powder samples are presented.